Journal of Alloys and Compounds 509 (2011) 99–104

Contents lists available at ScienceDirect

Journal of Alloys and Compounds

journal homepage: www.elsevier.com/locate/jallcom

Microwave-assisted synthesis and characterization of $Nd_{1.5}Mg_{17}Ni_{0.5}$–Fe_3O_4 hydrogen storage composite

Qian Li*, Li-Wen Ye, Jie Meng, Yang Liu, Kuo-Chih Chou

Shanghai Key Laboratory of Modern Metallurgy & Materials Processing, Shanghai University, Shanghai 200072, PR China

ARTICLE INFO

Article history:
Received 14 June 2010
Received in revised form 22 August 2010
Accepted 25 August 2010

Keywords:
Hydrogen absorbing materials
Metal hydrides
Powder metallurgy
Kinetics
Thermodynamic properties

ABSTRACT

This work reports the preparation of $Nd_{1.5}Mg_{17}Ni_{0.5}$–Fe_3O_4 hydrogen storage composite in a single mode 2.45 GHz microwave cavity. The physicochemical properties (thermodynamic and kinetic characteristics, hydrogen absorption/desorption properties, thermal behavior, phase composition and morphology) were characterized by pressure-composition isotherms, differential scanning calorimetry, X-ray diffraction, scanning electron microscope with an energy dispersive X-ray spectrometer, transmission electron microscopy, and laser granulometry. The proposed microwave synthesis, in contrast with conventional sintering method, offers rapid heating, makes homogenous composition and hence improves the hydrogen storage properties of the composite.

1. Introduction

The storage of large quantities of hydrogen under safe pressure is a key factor in establishing a hydrogen-based economy [1]. So a broad variety of materials are considered as potential hydrogen-storage materials [2] such as nanostructural carbon [3], tuning clathrate hydrates [4], metal organic frameworks [5], metal hydrides [6], lithium and sodium amidoboranes [7]. According to the International Energy Association's (IEA) feasibility study, the mobile hydrogen storage system can provide a gravimetric storage capacity larger than 5 wt.% of H_2, desorption temperature lower than 423 K and at least 1000 hydriding/dehydriding cycles life [8]. Magnesium is the only pure metallic element that can reversibly store more than 5 wt.% H in the form of metal hydride. It is the lightest of all engineering metals with a density of 1.74 g/cm^3 and the sixth most abundant element in the earth crust. However, its disadvantages are poor hydrogen sorption kinetic properties, high sorption temperature and high reactivity to oxidation. Many efforts have been made to improve its hydriding/dehydriding performance. For example, many elements such as V, Ti, Ni, Fe, Mn, Cu and Ag [9–11] have been selected as additives to magnesium. Among the addition of catalysts [6], pure transition metals [9] and oxides [12] are often reported. Re–Mg–Ni alloys always showed excellent hydrogen storage property. Xie et al. [13] prepared hydrogen storage alloys $Mg_{2-x}Nd_xNi$ (x = 0, 0.1, 0.2, 0.3) by vacuum induction melting under the high purity helium atmosphere and found that the substitution of Nd for Mg had obviously improved the hydrogen storage properties of Mg_2Ni. According to the results in literatures, transition metal oxides show higher potential. Oxides are cheap, and low amounts already have a substantial effect. Huang et al. [14] investigated iron oxides (Fe_2O_3, Fe_3O_4) as catalysts for improving hydrogen sorption in Mg-based materials and reported that the composite material containing Fe_3O_4 showed the higher hydrogen storage capacity than the material with Fe_2O_3 because of the reduction reaction between magnesium and iron oxides.

Additionally, the preparation of Mg-based composite is one of the key issues since it has strong influence on the microstructure, morphology and macro-properties of the material. The conventional heating method of thermal conduction from the outside to the inside of the sample need more time to heat specimens completely, cannot heat samples uniformly because of the thermal gradient and may lose much thermal energy during thermal conducting. A synthesis route encompassing encapsulation of subliming Mg by La from all sides has been adopted by Dutta and Srivastava [15], who melted La_2Mg_{17} intermetallic in a pre-baked quartz tube under an argon atmosphere with the help of a radio-frequency induction furnace. It is a pity that a special precaution coming from the very high Mg vapor pressure at the temperature of the melting point of La element was unreachable. It is well known that some external fields usually have significant effect on the properties of materials, especially for metal materials [16]. We recently carried out a feasibility study on synthesis of Mg–3 mol%$LaNi_3$ composite prepared under an external magnetic field and preparation of Mg_2NiH_4 made by microwave-assisted activation synthesis from

* Corresponding author. Tel.: +86 21 56334045; fax: +86 21 56338065.
E-mail addresses: qian246@hotmail.com, shuliqian@shu.edu.cn (Q. Li).

0925-8388/$ – see front matter © 2010 Elsevier B.V. All rights reserved.
doi:10.1016/j.jallcom.2010.08.123

micro-particles [17,18]. Compared with conventional processes, sintering under an external magnetic field and microwave field has attracted increasing attention due to their significant advantages in material processing. Microwaves allow volumetric heating of materials. Microwave energy transforms into heat inside the material, which results in significant reduction of energy and processing time. Investigations on microwave sintering of metallic materials primarily focused on ferrous [19], copper-based alloys [20], aluminum and its composites [21] have been reported and the results indicated that microwave sintering was superior to the conventional sintering in elevating sintered density and improving microstructural uniformity.

The aim of the present study has two aspects (i) to evaluate the feasibility of microwave sintering approach for synthesizing $Nd_{1.5}Mg_{17}Ni_{0.5}$–Fe_3O_4 composite and (ii) to investigate the effects of microwave sintering on the microstructure, hydriding/dehydriding thermodynamic and kinetic properties of this composite.

2. Experimental details

2.1. Preparation

The initial materials used in the experiments were Nd (>99.5% pure, ~200 mesh), Mg (>99.5% pure, ~400 mesh), Ni (>99.5% pure, <400 mesh) and Fe_3O_4 (>99.5% pure, ~200 mesh) powders. The as-received elemental powders of Nd, Mg and Ni with the atom ratio as 1.5:17:0.5 were mixed with 5 wt.% Fe_3O_4 powder. All the powders were milled in planetary ball milling with 60 rpm before sintering. To prevent oxidation during ball milling process, the samples contained in ball milling tanks were put in the glove box in a gas mixture of 95%Ar + 5%H_2. The tankage in this experiment is 80 cm^3 and the weight ratio of grinding media to material is 8:1. They were pressed under 300 MPa for 5 min into compact with dimension of 15 mm diameter and 5 mm thickness by a uniaxial single-acting press.

To verify that microwaves contribute effectively to the heating of the samples, the tests of sintering with and without microwave furnace were performed. The composite synthesized without microwave field is labeled as specimen 1 (S1) while the other with external microwave field is specimen 2 (S2). Microwave sintering was carried out in a microwave furnace with a frequency of 2.45 GHz microwave generator, a power output continuously adjustable from 0 to 3 kW, a cylindrical single-mode tuneable applicator, and a computer control system. Temperature was measured by an infrared pyrometer with an emissivity of 0.75. The compact was placed in the center of alumina fiber insulations with supplementary SiC heater. The alumina fiber insulations were used and mounted encircling the compact to inhibit the heat loss. The heating rate was adjusted by changing the output power. The whole sintering process was in high purity argon under an ambient pressure. Specimen 2 was sintered under the external microwave field with the heating rate of 40 K/min and was kept at 943 K for 15 min with flowing 0.1 MPa Ar. Similarly, sintering was conducted in a tubular resistance furnace without microwave field for specimen 1. The products were cooled to room temperature and crushed into micro-particles for the characterization. Fig. 1 shows a schematic illustration of the experimental equipment. It mainly consists of a microwave oven and a heat preservation system.

2.2. Characterization

The samples were activated for 3 times (under 4.0 MPa H_2, absorption for 60 min, and desorption in vacuum for 60 min at 573 K). The pressure-composition isotherm (PCT) and kinetic properties were measured by a volumetric method according to Sievert's law using automatic apparatus from SUZUKI HOKAN Co., Ltd. in Japan. The structures of the samples were analyzed by X-ray diffraction (XRD) and their morphologies were studied by scanning electronic microscopy (SEM) with an energy dispersive X-ray analysis system (EDS). The TEM image of product was obtained at the accelerating voltage of 200 kV. TEM samples were prepared by the room temperature organic (RTO) method [22]. Size measurements were performed using a Malvern Mastersizer hydro 2000S in liquid ethanol media. The sample (20 mg) was dispersed in ethanol using an ultrasonic device (80 kHz, 150 W, 20 min). Differential scanning calorimeter (DSC) measurements were carried out on approximately 30 mg of as-prepared sample at a heating rate of 6 K/min from 298 to 773 K and the maximum temperature was kept for 120 min with flowing 0.1 MPa Ar at a rate of 100 ml/min.

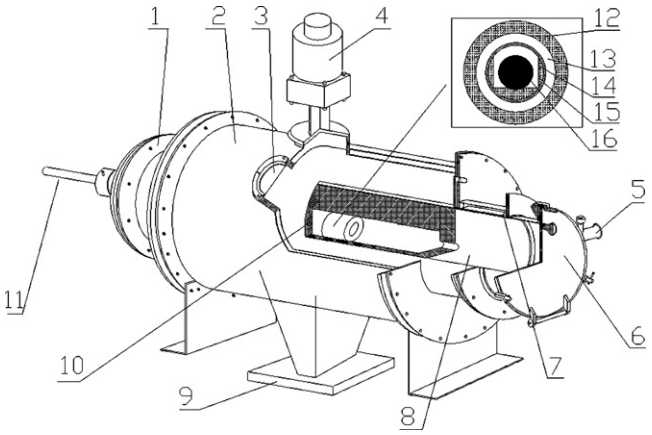

Fig. 1. Schematic illustration of apparatus for the microwave furnace: (1) venthole, (2) furnace body, (3) peephole, (4) agitator, (5) vacuum system, (6) furnace door, (7) O-ring seal, (8) furnace tube, (9) microwave feed-in, (10) insulating course, (11) infrared pyrometer, (12) insulation fiber, (13) alumina insulation, (14) corundum crucible, (15) supplementary SiC heater, and (16) sample.

3. Results and discussion

3.1. The structural characteristics

The XRD patterns of specimens 1 and 2 before and after hydriding reaction are shown in Fig. 2. Apart from the starting iron oxides (Fe_3O_4, JCPDS 19-0629, 28-0491) in the composites, peaks of the

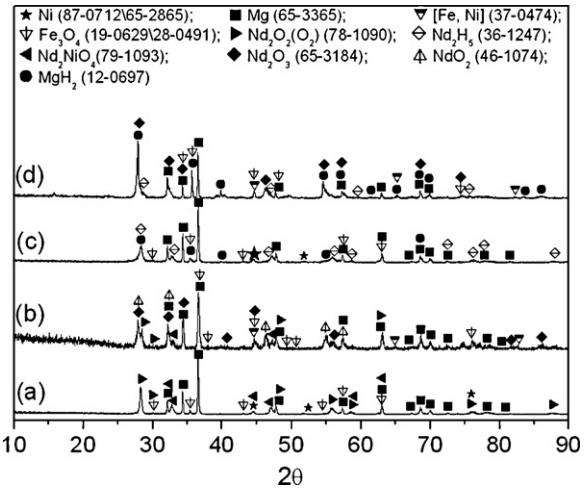

Fig. 2. X-ray diffraction patterns of $Nd_{1.5}Mg_{17}Ni_{0.5}$–Fe_3O_4 prepared with and without external microwave field before (a for S1, b for S2) and after (c for S1, d for S2) hydride activation.

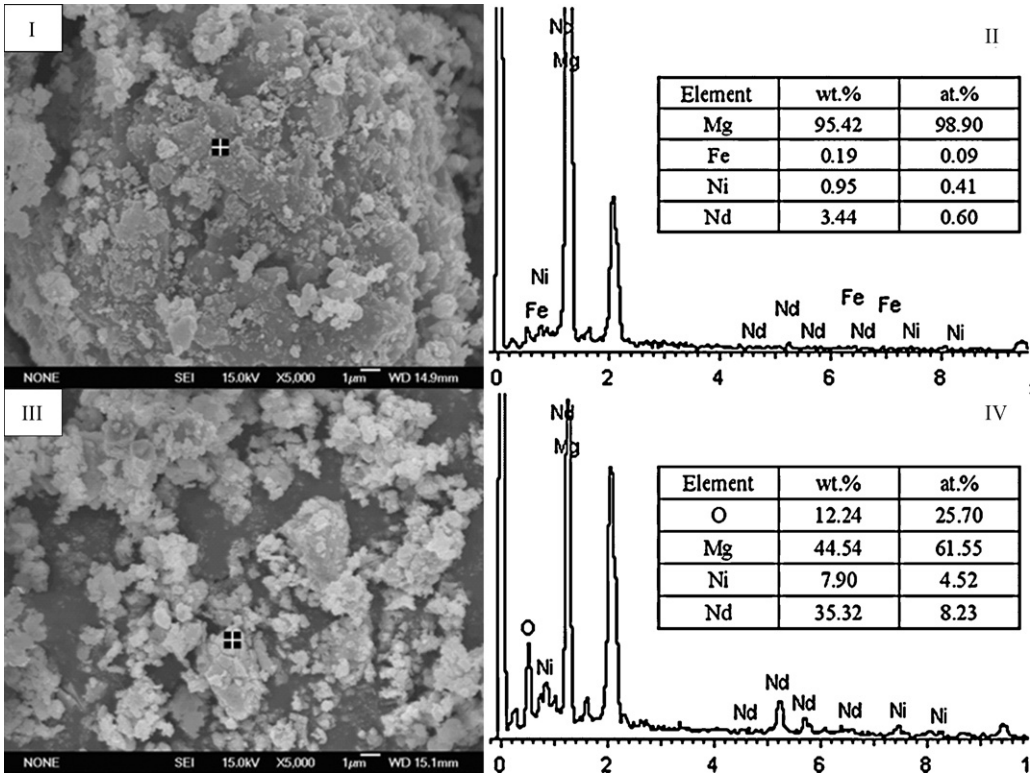

Fig. 3. SEM and EDS observation of $Nd_{1.5}Mg_{17}Ni_{0.5}$–Fe_3O_4 prepared under the different conditions after hydride activation: (I, II) without microwave field and (III, IV) with microwave field.

hexagonal Mg (JCPDS, 63-3655) phase, nickel (JCPDS, 87-0712, 65-2865) and Nd oxides are visible in both patterns (Fig. 2a and b) before hydriding reaction. After hydriding reaction, the conventionally sintered sample (S1) is mainly composed of the hexagonal Mg and some tetragonal β-MgH_2 (JCPDS, 12-0697) phase, whereas the microwave sintered sample (S2) contains much more the tetragonal β-MgH_2 and just a little hexagonal Mg, which means that after hydriding reaction the Mg phase of specimen 2 reacted with hydrogen more fully than that of specimen 1. The metal oxides, such as Fe_3O_4, Nd_2NiO_4 (JCPDS, 79-1093), $Nd_2O_2(O_2)$ (JCPDS, 78-1090), Nd_2O_2 (JCPDS, 46-1074) and Nd_2O_3 (JCPDS, 65-3184), are showed and the peaks of metal oxides are obvious in specimen 2 (Fig. 2b and d). It is well known that metal oxide catalysts have a positive effect on the sorption behavior of Mg-based hydrogen storage materials [14,23]. And it was reported that the application of microwave field decreased activation energy of chemical reaction [24], so more various metal oxides in specimen 2 than those in specimen 1 were in favor of the hydriding reaction and hence the more MgH_2 phase were appearance because of the catalysis of metal oxides.

Fig. 3 shows the results of SEM and EDS analysis of the surface of $Nd_{1.5}Mg_{17}Ni_{0.5}$–Fe_3O_4. Comparing Fig. 3I with Fig. 3III, we find that the specimen prepared in microwave field is distributed uniformly with average diameter of 1–5 μm. And the specimen 1 has larger particle size (average diameter of 5–20 μm) and its surface shows the clusters with smaller particles. The EDS analysis of the surface compositions for the two specimens shows that Mg is the main composition in both specimens, but the fractions of O on the surface of the specimen 1 are smaller than those of the specimen 2, which agrees well with the XRD analysis result. The presence of clusters in specimen 1, as seen in Fig. 3, indicates that the agglomeration may cause the inhomogeneous composition in these composites. Fig. 4 also shows the TEM and HRTEM panorama of the specimen 2 prepared under the microwave field. The TEM

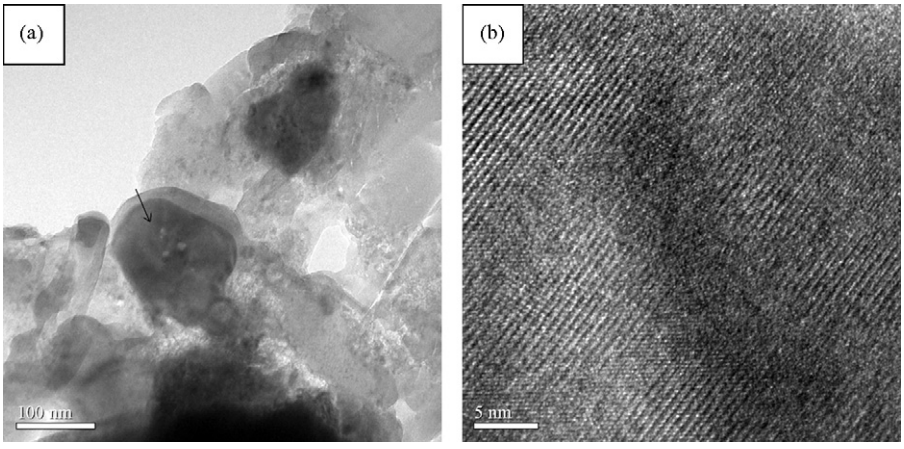

Fig. 4. TEM and high-resolution TEM micrographs of $Nd_{1.5}Mg_{17}Ni_{0.5}$–Fe_3O_4 composite prepared under microwave field: (a) TEM panorama and (b) HRTEM panorama.

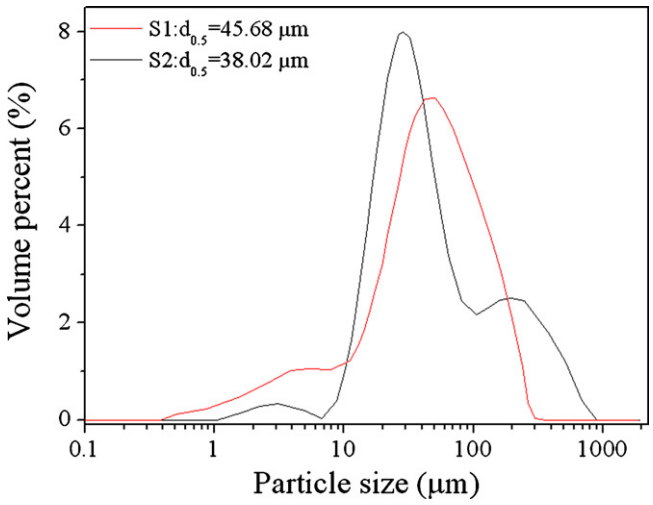

Fig. 5. Particle size distribution of different samples.

images show a homogeneous crystallite size distribution with average crystallite size smaller than 150 nm. The HRTEM bright field image seen in Fig. 4 shows the presence of dark particles embedded in the Mg matrix. The homogeneous composition shown in the HRTEM panorama agrees well with the SEM analysis results. As is thought, the microwave heating is rapid and increases the rate of solid phase diffusions. And the homogeneous composition could improve the properties of the hydrogen storage materials.

The particle size distribution of the $Nd_{1.5}Mg_{17}Ni_{0.5}$–Fe_3O_4 composite was obtained by means of granulometric measurements and shown in Fig. 5. The median of the distribution changes from 45.68 μm for specimen 1 to 38.02 μm for specimen 2. The tendency of the particle size change is consistent with the information provided by SEM results. The comparison of the median size under different conditions suggests that the effect of the microwave field on the size distribution of the particles is obvious. The observed results show that the particle size was decreased under the external microwave field.

3.2. Thermodynamic properties

Pressure-composition isotherm curves at 553–623 K for the specimens 1 and 2 are plotted in Fig. 6. This figure shows that the hydrogen storage capacity of specimen 1 is only 2.2 wt.% at the temperature ranging from 553 to 623 K, the specimen 2 sintered by microwave energy has a high hydrogen storage capacity of 4.48–4.60 wt.% at the same temperature with a low, flat and wide plateau of hydrogen sorption, and most of the total hydrogen absorbed can desorb above 553 K and 0.1 MPa. The discrepancy of hydrogen storage capacity between the specimen 1 and the specimen 2 can be explained by the fact of the different preparation of the two specimens. Compared with the specimen 1 sintered without microwave field, the specimen 2 prepared in microwave field has smaller particles and more homogeneous composition, which made hydrogenation reactants contacting with each other more fully. But in specimen 1 prepared without microwave field the coarse particles and inhomogeneous composition made Mg phase not absorbing hydrogen completely. So the discrepancy of hydrogen storage capacity between two specimens was visible.

Several PCT curves of hydrogen absorption and desorption were measured in range of temperature from 553 to 623 K. The enthalpies of hydrogen absorption and desorption (ΔH) were calculated using the values of the plateau pressures (p) of absorption and desorption isotherms as a function of temperature (T) by the Van't Hoff relation [1]:

$$\ln(p) = \frac{\Delta H}{RT} - \frac{\Delta S}{R} \quad (1)$$

where ΔS is the entropy of reaction and R is the universal gas constant. The enthalpies of absorption and desorption were calculated from the slope of the linear interpolation of the Van't Hoff plot (Fig. 6).

The correlation coefficient of the linear regression was 0.998. Table 1 summarizes the equilibrium plateau pressure, entropy, enthalpy and Van't Hoff equations of hydriding (H) and dehydriding (D) reactions at different temperatures for the specimens.

In order to evaluate the thermal characteristics of the samples prepared under microwave field, the differential scanning

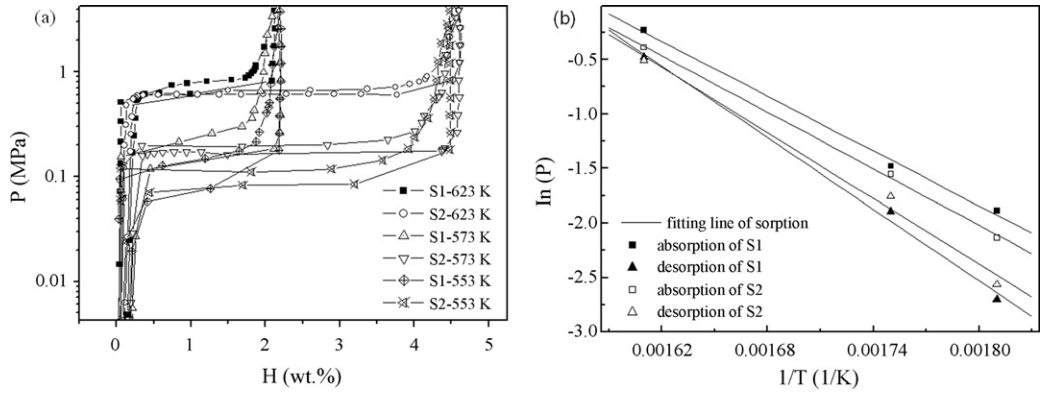

Fig. 6. (a) PCT curves of different samples at different temperatures and (b) Van't Hoff plot of the hydrogen absorption and desorption of $Nd_{1.5}Mg_{17}Ni_{0.5}$–Fe_3O_4 composite.

Table 1
Equilibrium plateau pressure, entropy, enthalpy and Van't Hoff equations of hydriding (H) and dehydriding (D) at different temperatures.

Samples	T (K)	P_H (MPa)	P_D (MPa)	C_H (wt.%)	C_D (wt.%)	Hydriding	Dehydriding
S1	553	0.151	0.067	2.21	2.04	$\Delta H = -69.7 \pm 4.0$ kJ/mol	$\Delta H = 90.9 \pm 6.4$ kJ/mol
	573	0.228	0.150	2.22	2.00	$\Delta S = -110.5 \pm 6.6$ J/mol K	$\Delta S = 143.0 \pm 10.8$ J/mol K
	623	0.792	0.620	2.23	2.08	$\ln(P) = -8389.9/T + 13.3$	$\ln(P) = -10937.6/T + 17.2$
S2	553	0.118	0.077	4.48	4.47	$\Delta H = -71.8 \pm 2.5$ kJ/mol	$\Delta H = -83.3 \pm 8.6$ kJ/mol
	573	0.211	0.173	4.60	4.50	$\Delta S = -112.2 \pm 4.2$ J/mol K	$\Delta S = 130.5 \pm 15.0$ J/mol K
	623	0.676	0.602	4.60	4.52	$\ln(P) = -8634.5/T + 13.5$	$\ln(P) = -10025.6/T + 15.7$

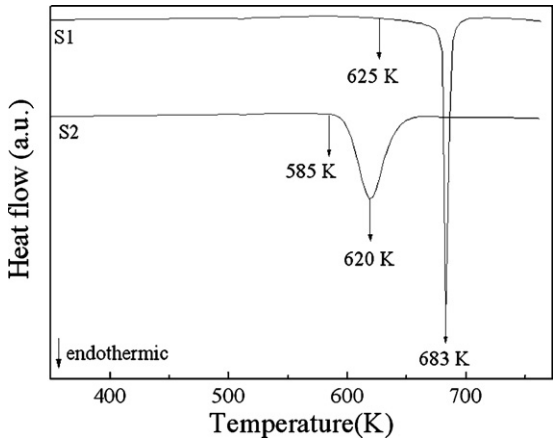

Fig. 7. DSC curves of the different samples measured in the range of 298–773 K at a heating rate of 6 K/min under 0.1 MPa Ar.

calorimeter (DSC) was applied in the dehydrogenation. Fig. 7 shows the DSC curves of the hydrogenated samples at a heating rate of 6 K/min and under 0.1 MPa Ar. There is only one desorption peak in the curve of specimens 1 and 2, which resulted from the decomposition of MgH_2 into $Mg + H_2$. From the DSC result in Fig. 7, the onset temperatures of desorption are 625 K for S1 and 585 K for S2, respectively. The temperatures of endothermic peaks are around 620 K for S2 and 683 K for S1. Compared with the specimen 1, the onset temperature of hydrogen sorption and the temperature at the dehydriding peak of specimen 2 decreased dramatically. Therefore, it is easier to release hydrogen from the specimen 2, which can be attributed to the homogeneous composition and small particles in S2 prepared under microwave field. As our previous work, the microwave field may impose positive effect on the thermodynamic properties of hydrogen storage alloys [18].

3.3. Kinetic properties

The rates of hydriding/dehydriding reactions are also a key property of the hydrogen storage composite. Fig. 8 presents the kinetic curves of hydrogen sorption for different samples in the range of temperature from 553 to 623 K. It was observed that the rates of hydriding/dehydriding reactions for the two specimens increased with the increasing temperature from 553 to 623 K. The kinetic properties of the samples under the microwave were improved significantly. From the kinetic curves of hydrogen absorption in temperature range from 553 to 623 K, it shows that the specimen 2 prepared under microwave field can absorb more hydrogen than the specimen 1 prepared without microwave field. From the kinetic curves of hydriding reaction, we know the specimen 2 could absorb more than 60% hydrogen of the maximum hydrogen storage capacity, but the specimen 1 just absorb about 50% hydrogen. And in 200 s, the specimen 2 can absorb hydrogen more than 1.74 wt.%, but the specimen 1 can only absorb 0.73 wt.% hydrogen at 623 K. From the kinetic curves of hydrogen desorption, we also can find that the rate of desorption reaction increased with the increase of the temperature from 553 to 623 K. And at the same temperature, the specimen 2 can release more hydrogen than the specimen 1. For instance, in 200 s, the specimen 2 can release 1.25 wt.% hydrogen, but the specimen 1 just released 0.30 wt.% hydrogen at 573 K. From the results, it can be found that the kinetic properties of microwave sintered specimen were better than that of the specimen prepared without microwave field. The microwave heating for 15 min, which was uniform and volumetric heating, could increase the rate of solid phase diffusion. So the distribution of solid phase was homogeneous in the microwave sintered specimen and then it will be beneficial to the hydrogen sorption reaction.

As is known, one important characteristic of microwave heating is that the entire volume of particles get heated up since generally the microwave can penetrate the particles completely [24]. Different from the conventional heating method, the microwave heating is very rapid and has the minimum thermal gradients, which is favor of the solid phase diffusion during sintering. So the microwave sintered specimen has smaller particle size and more homogenous composition. The microwave field also affects the physical and chemical reaction among the composition, such as decreasing activation energy of chemical reaction [24]. So in the microwave sintered specimen there are more various metal oxides formed. All the microstructures differed from those of conventional sintered specimen make it better hydrogen storage properties, such as higher hydrogen storage capacity and better kinetics properties of hydrogen storage.

4. Conclusions

Based on the microwave-assisted synthesis technique, the $Nd_{1.5}Mg_{17}Ni_{0.5}$–Fe_3O_4 composite was synthesized. With the special heating method of microwave sintering, the small particle, homogenous composition and various metal oxides were formed in the microwave sintered $Nd_{1.5}Mg_{17}Ni_{0.5}$–Fe_3O_4 composite. By analyzing the microstructure, composition and morphology of the composites prepared by microwave sintering and conventional sintering methods, the positive effect of microwave sintering on their hydriding/dehydriding properties has been obtained. And in comparison with the conventionally sintered sample, the microwave sintered $Nd_{1.5}Mg_{17}Ni_{0.5}$–Fe_3O_4 composite demon-

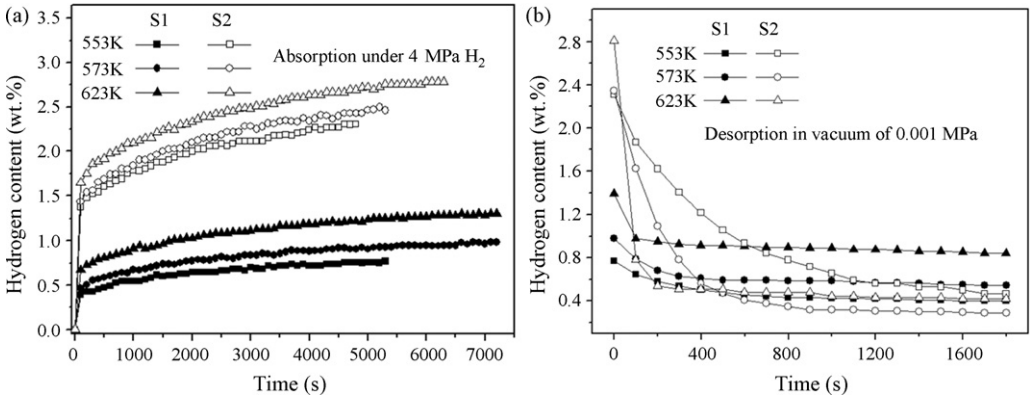

Fig. 8. (a) Hydrogen absorption curves of $Nd_{1.5}Mg_{17}Ni_{0.5}$–Fe_3O_4 composite under 4 MPa H_2 and (b) hydrogen desorption curves of $Nd_{1.5}Mg_{17}Ni_{0.5}$–Fe_3O_4 composite in vacuum at different temperatures.

strated the improved thermodynamic and kinetic properties of hydrogen absorption and desorption.

Acknowledgements

Financial supports from the National Natural Science Foundation of China (50804029), a Foundation for the Author of National Excellent Doctoral Dissertation of P.R. China (200746) and the Program for Changjiang Scholars and Innovative Research Team in University (IRT0739) are gratefully acknowledged.

References

[1] L. Schlapbach, A. Züttel, Nature 414 (2001) 353–358.
[2] I.P. Jain, P. Jain, A. Jain, J. Alloys Compd. 503 (2010) 303–339.
[3] Y. Kojima, Y. Kawai, A. Koiwai, N. Suzuki, T. Haga, T. Hioki, et al., J. Alloys Compd. 421 (2006) 204–208.
[4] H. Lee, J.W. Lee, D.Y. Kim, J. Park, Y.T. Seo, H. Zeng, et al., Nature 434 (2005) 743–746.
[5] J.L.C. Rowsell, O.M. Yaghi, J. Am. Chem. Soc. 128 (2006) 1304–1315.
[6] B. Sakintuna, F. Lamari-Darkrim, M. Hirscher, Int. J. Hydrogen Energy 32 (2007) 1121–1140.
[7] Z.T. Xiong, C.K. Yong, G.T. Wu, P. Chen, W. Shaw, A. Karkamkar, et al., Nature 7 (2008) 138–141.
[8] S. Satyapal, J. Petrovic, C. Read, G. Thomas, G. Ordaz, Catal. Today 120 (2007) 246–256.
[9] M. Pozzo, D. Alfè, Int. J. Hydrogen Energy 34 (2009) 1922–1930.
[10] S.N. Kwon, S.H. Baek, D.R. Mumm, S.H. Hong, M.Y. Song, Int. J. Hydrogen Energy 33 (2008) 4586–4592.
[11] Q. Li, Q. Lin, L.J. Jiang, K.C. Chou, F. Zhan, Q. Zheng, et al., J. Alloys Compd. 359 (2003) 128–132.
[12] K.-F. Aguey-Zinsou, T. Nicolaisen, J.R. Ares Fernandez, T. Klassen, R. Bormanna, J. Alloys Compd. 434–435 (2007) 738–742.
[13] D.H. Xie, P. Li, C.X. Zeng, J.W. Sun, X.H. Qu, J. Alloys Compd. 478 (2009) 96–102.
[14] Z.G. Huang, Z.P. Guo, A. Calka, D. Wexler, C. Lukey, H.K. Liu, J. Alloys Compd. 422 (2006) 299–304.
[15] K. Dutta, O.N. Srivastava, Int. J. Hydrogen Energy 15 (1990) 341–344.
[16] K. Naplocha, K. Granat, J. Alloys Compd. 480 (2009) 369–375.
[17] Q. Li, K.D. Xu, K.C. Chou, X.G. Lu, J.Y. Zhang, G.W. Lin, Intermetallics 15 (2007) 61–68.
[18] Y. Liu, Q. Li, G.W. Lin, K.C. Chou, K.D. Xu, J. Alloys Compd. 468 (2009) 455–461.
[19] R. Roy, D. Agrawal, J. Cheng, S. Gedevanishvili, Nature 399 (1999) 668–670.
[20] S.D. Luo, J.H. Yi, Y.L. Guo, Y.D. Peng, L.Y. Li, J.M. Ran, J. Alloys Compd. 473 (2009) L5–L9.
[21] K. Naplocha, K. Granat, J. Alloys Compd. 486 (2009) 178–184.
[22] K.M. Fang, Z. Lin, K. Fang, China Particuol. 1 (2003) 88–90.
[23] M.Y. Song, D.R. Mumm, S.N. Kwon, S.H. Hong, J.S. Bae, J. Alloys Compd. 416 (2006) 239–244.
[24] K.J. Rao, P.D. Ramesh, Bull. Mater. Sci. 18 (1995) 447–465.